IEEE Access
Multidisciplinary | Rapid Review | Open Access Journal

Received March 24, 2020, accepted April 13, 2020, date of publication April 24, 2020, date of current version May 8, 2020.

Digital Object Identifier 10.1109/ACCESS.2020.2990169

Wideband Printed Ridge Gap Rat-Race Coupler for Differential Feeding Antenna

ISLAM AFIFI[1,2], (Graduate Student Member, IEEE), AND ABDEL RAZIK SEBAK[1], (Life Fellow, IEEE)

[1]Department of Electrical and Computer Engineering, Concordia University, Montreal, QC H4B 1R6, Canada
[2]Engineering Mathematics and Physics Department, Cairo University, Giza 12613, Egypt

Corresponding author: Islam Afifi (i_afifi@encs.concordia.ca)

ABSTRACT In this paper, a wideband 3 dB hybrid 180° rat-race coupler is introduced in the printed ridge gap waveguide technology. It has simultaneous wide matching and isolation bandwidth with low output amplitude imbalance. It operates in the millimeter wave band from 25.8 to 34.2 GHz (27.96%) with 15 dB return loss and isolation, and ±0.5 dB output amplitude imbalance. The proposed design employing an open stub at the middle of the $3\lambda/4$ branch line and quarter wavelength lines at all the ports of the coupler. The objective of the added open stub is to separate the output ports amplitudes around the -3 dB level by certain values depending on the required amplitude imbalance. The analytical derivation for the role of the added open stub is presented along with a parametric study on its effect on amplitude imbalance, matching, and isolation. This results in having two intersection points for the output ports instead of one of the conventional coupler and hence the amplitude imbalance bandwidth increases. The objective of the added quarter wavelength lines is to improve the matching and isolation bandwidths. First, the conventional rat-race coupler is presented and a bandwidth of 14.25% at 30 GHz is achieved. After that the rat-race with the added quarter wavelength lines is presented to illustrate the objective of the added quarter wavelength lines and a bandwidth of 19.44% is achieved. Finally, the rat-race with the quarter wavelength lines and the added stub is presented and a prototype is fabricated and measured. The s-parameters measurements are in a good agreement with the simulated ones.

INDEX TERMS Printed ridge gap, rat race coupler, millimeter wave components.

I. INTRODUCTION

The Millimeter wave (mmw) band has gained a great attention in the research society. It opens up a broadband spectrum for a wide range of applications such as the next generation (5G) communication, automotive radar, remote sensing and security imaging [1]–[4]. Therefore, there is a need for new mmw devices to meet such huge spectrum. It is well-known that the conventional microstrip components is lossy at this frequency band. Thus, other waveguide structures become mandatory. One of the promising prototyping technologies is the ridge gap waveguide (RGW), where the propagating mode is the QTEM mode that has a small signal distortion. Another advantage of the RGW structure is that the wave propagates in air. Therefore, dielectric losses are eliminated. Moreover, the structure is closed which eliminates the radiation losses. There are two types of the ridge gap waveguide based on the fabrication technology. The first is the metal RGW introduced by Zaman *et al.* [5], Kildal [6], and Kildal *et al.* [7] where the computer numerical control (CNC) machining is used in the fabrication. The second is the printed RGW (PRGW) [8] where the printed circuit board (PCB) technology is used. RGW and PRGW technologies have been used in the design and implementation of several components such as couplers and antennas at different frequencies including 15 GHz [9], [10], 30 GHz [11]–[15], and 60 GHz [16]. In this paper, PRGW is used to implement a wideband, low cost, and light-weight rat-race coupler compared to the metallic one. More importantly, it is easily integrated with other devices and chips on PCB boards.

Rat-race coupler has important role in many microwave circuits. It provides equal power division with in-phase and out of phase characteristics, depending on the feeding port. It is used in mixers and differential feeding network. It has been implemented in different technologies such as microstrip line, substrate integrated waveguide (SIW), and ridge gap

The associate editor coordinating the review of this manuscript and approving it for publication was Antonino Orsino.

waveguide (RGW). Several techniques to improve the bandwidth and reduce the size are used. In [17], a full optimized rat-race coupler with quarter wavelength transformers at all ports is presented where a maximum bandwidth of 50.6% is achieved. However the impedance ratio is high (1:8.75) which leads to fabrication challenges. A technique to decrease the size and increase the bandwidth is implemented by using a 180° phase inverter with only one quarter wavelength section instead of the $3\lambda/4$ branch, using short lines reduces the frequency dependency of the rat-race coupler. This technique was first introduced theoretically by S. March in 1968 [18], where a shorted coupled line coupler section with $\lambda/4$ length is used instead of the $3\lambda/4$ section. In [19], two quarter wavelength coupled line coupler are added to the structure in [18] to have different impedances at two ports of the rat-race coupler with wide bandwidth. The same technique is implemented in the coplanar waveguide [20], [21], finite-ground-plane coplanar waveguide (FGCPW) [22], and inter digit coplanar waveguide [23]. This technique needs uniplanar waveguide structure that facilitates making the phase inverter either by using bonding wires or conductive tape without increasing the size of the structure. In [24], this technique is combined with adding quarter wavelength transformers at all ports to further increase the bandwidth. Also, replacing the $3\lambda/4$ by a $\lambda/4$ left handed transmission line gives the same effect [25]–[27]. Moreover, lumped elements are used for size reduction by replacing the transmission lines [28]–[30] or loading the transmission lines and reduce its electrical length [31]. Also, slow wave waveguides have been used to reduce the size as in [32], [33]. Finally, cascading of rat-race couplers is used to have a wideband as in [34]. These techniques are valid for low operating frequencies as there is enough area to build left handed transmission line, slow wave structures, or to use lumped elements. However, at high frequencies, the devices become very small and there is no enough area to build artificial transmission lines or to use lumped elements with the current PCB technology.

For high frequency devices, new guiding structure technologies such as substrate integrated waveguide (SIW) and ridge gap waveguide are considered good candidates. The SIW has been used to build rat-race coupler [35]. However, as the propagating mode is TE_{10} and the width of the waveguide is large, the $\lambda/4$ section can not be realized and $5\lambda/4$ is used instead. This increases the frequency dependency of the structure and the bandwidth is only 10%. Then it has been optimized in [36] to reach 30%. Several techniques has been used to reduce the over all size of the SIW rat-race such as using half mode SIW [37], folded SIW [38] or ridge SIW with slow wave [39]. All of these works suffer from the dielectric losses in SIW technology. Considering the ridge gap waveguide, to the authors' best knowledge, only one article has been found [40] in metal RGW technology and using conventional rat-race with only 12.1% bandwidth around 16.5 GHz.

In this paper, a wideband rat-race coupler is designed at the millimeter wave band using the PRGW technology. The addition of open stub and quarter wavelength transformers has greatly improved the impedance, isolation, and amplitude imbalance bandwidths. First, the general equations of the proposed coupler are presented along with a parametric study to show the effect of the added stub on the amplitude imbalance, and matching and isolation bandwidths. Second, the conventional rat-race coupler is designed in the PRGW to show its performance in this new technology. Third, the rat-race with the added quarter wavelengths is presented as a first step for a wide bandwidth (increasing the matching and isolation bandwidths). Also, multiple quarter wavelength transforms can be used to have different input and output impedances as in [19]. Finally, rat-race with the quarter wavelengths and the open stub at the middle of the $3\lambda/4$ branch line is presented. The operating bandwidth is determined by having the return loss and the isolation better than 15 dB, and a coupling imbalance less than 1 dB (peak-to-peak).

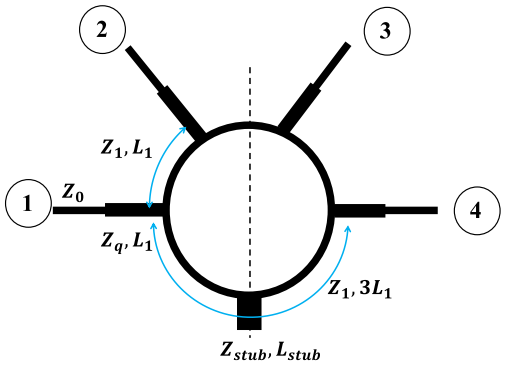

FIGURE 1. Geometry of the proposed Rat race coupler.

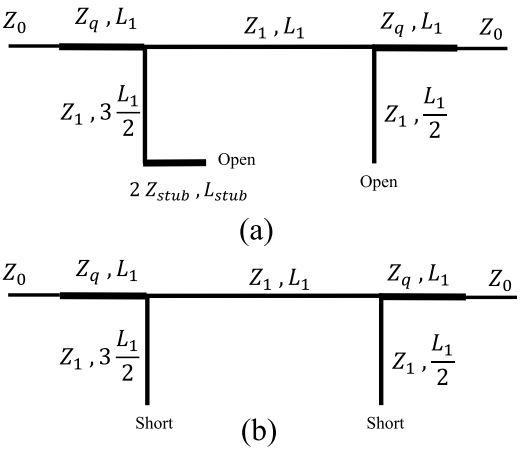

FIGURE 2. Equivalent even and odd circuits of the proposed rat race. (a) Even mode circuit model. (b) Odd mode circuit model.

II. THEORY

In this section, the general geometry of the rat race coupler with quarter wave transformers and a stub at the middle of the $3\lambda/4$ branch line is analyzed using odd and even mode analysis. The geometry of the proposed rat race is shown in Fig. 1 and the even and odd equivalent circuits are shown in Fig. 2. The s-parameters of the rat race is calculated from the

even and odd analysis as follows [42].

$$S_{11} = \frac{S_{11e} + S_{11o}}{2} \tag{1}$$

$$S_{21} = \frac{S_{21e} + S_{21o}}{2} \tag{2}$$

$$S_{31} = \frac{S_{21e} - S_{21o}}{2} \tag{3}$$

$$S_{41} = \frac{S_{11e} - S_{11o}}{2} \tag{4}$$

where S_{11e},S_{21e}, S_{11o}, and S_{21e} are calculated by applying the even and odd symmetry respectively on the rat race. The even symmetry leaves open stubs while the odd symmetry leaves short stubs. The ABCD matrices of different sections of the rat race for even symmetry are

$$ABCD_{1e} = \begin{bmatrix} \cos(\beta L_1) & jZ_q \sin(\beta L_1) \\ jY_q \sin(\beta L_1) & \cos(\beta L_1) \end{bmatrix} \tag{5}$$

$$ABCD_{2e} = \begin{bmatrix} 1 & 0 \\ \frac{Z1+2Z_{stub}\cot(\beta L_{stub})\tan(3\beta L_1/2))}{Z_1(-2jZ_{stub}\cot(\beta L_{stub})+jZ_1\tan(3\beta L_1/2))} & 1 \end{bmatrix} \tag{6}$$

$$ABCD_{3e} = \begin{bmatrix} \cos(\beta L_1) & jZ_1 \sin(\beta L_1) \\ jY_1 \sin(\beta L_1) & \cos(\beta L_1) \end{bmatrix} \tag{7}$$

$$ABCD_{4e} = \begin{bmatrix} 1 & 0 \\ jY_1 \tan(\beta L_1/2) & 1 \end{bmatrix} \tag{8}$$

the total ABCD matrix for the even mode is given by

$$ABCD_{even\ total} = ABCD_{1e}\ ABCD_{2e}\ ABCD_{3e}\ ABCD_{4e}\ ABCD_{1e} \tag{9}$$

For the odd mode analysis, the second and forth ABCD matrix are

$$ABCD_{2o} = \begin{bmatrix} 1 & 0 \\ -jY_1 \cot(3\beta L_1/2) & 1 \end{bmatrix} \tag{10}$$

$$ABCD_{4o} = \begin{bmatrix} 1 & 0 \\ -jY_1 \cot(\beta L_1/2) & 1 \end{bmatrix} \tag{11}$$

The total ABCD matrices for the odd case is

$$ABCD_{odd\ total} = ABCD_{1e}\ ABCD_{2o}\ ABCD_{3e}\ ABCD_{4o}\ ABCD_{1e} \tag{12}$$

From these general equations for the proposed rat race, the conventional rat race is obtained by making $Z_q = Z_0$, $Z_1 = \sqrt{2}Z_0$, and $L_{stub} \simeq 0$. The rat race with quarter wave transformers is obtained by making $Z_q = Z_0/\sqrt[4]{2}$, $Z_1 = Z_0$ and $L_{stub} \simeq 0$.

In order to illustrate the effect of the added stub on the amplitude imbalance, we take $Z_{stub} = \frac{1}{\sqrt{2}}Z_0$,and $Z_q = Z_0$. Therefore the $ABCD_{2e}$ can be written as

$$ABCD_{2e} = \begin{bmatrix} 1 & 0 \\ jY_1 \tan\left(\beta\left(\frac{3L_1}{2} + L_{stub}\right)\right) & 1 \end{bmatrix} \tag{13}$$

For small value of L_{stub} and at the center frequency,

$$\tan\left(\beta\left(\frac{3L_1}{2} + L_{stub}\right)\right) = \tan\left(\frac{3\pi}{4} + \Delta\theta\right) \tag{14}$$

where $\Delta\theta = \beta L_{stub}$, and using the trigonometric Identity that

$$\tan(a+b) = \frac{\tan a + \tan b}{1 - \tan a \tan b} \tag{15}$$

then

$$\tan\left(\frac{3\pi}{4} + \Delta\theta\right) \approx \frac{\Delta\theta - 1}{\Delta\theta + 1} \tag{16}$$

After that we substitute in the ABCD matrix and get the s-parameters as follows

$$S_{11} = \frac{\frac{1}{2}\Delta\theta(1 + j2\sqrt{2})}{-2\Delta\theta + j\sqrt{2}(\Delta\theta + 2)} \tag{17}$$

$$S_{21} = \frac{2 + \frac{3}{2}\Delta\theta + j\frac{1}{\sqrt{2}}\Delta\theta}{-2\Delta\theta + j\sqrt{2}(\Delta\theta + 2)} \tag{18}$$

$$S_{31} = \frac{\frac{1}{2}\Delta\theta(1 - j\sqrt{2})}{-2\Delta\theta + j\sqrt{2}(\Delta\theta + 2)} \tag{19}$$

$$S_{41} = \frac{-2 - \frac{1}{2}\Delta\theta}{-2\Delta\theta + j\sqrt{2}(\Delta\theta + 2)} \tag{20}$$

By taking the absolute values, Equations (21) to (24) are obtained.

$$|S_{11}|^2 = \Delta\theta^2 \frac{2.25}{6\Delta\theta^2 + 8\Delta\theta + 8} \tag{21}$$

$$|S_{21}|^2 - 1/2 = \Delta\theta \frac{2 - 0.25\Delta\theta}{6\Delta\theta^2 + 8\Delta\theta + 8} \tag{22}$$

$$|S_{31}|^2 = \Delta\theta^2 \frac{0.75}{6\Delta\theta^2 + 8\Delta\theta + 8} \tag{23}$$

$$|S_{41}|^2 - 1/2 = -\Delta\theta \frac{2.75\Delta\theta + 2}{6\Delta\theta^2 + 8\Delta\theta + 8} \tag{24}$$

These equations illustrate that the amplitude of S_{21} is greater than $\frac{1}{\sqrt{2}}$ and increase with proportion to the added stub length. Also, the amplitude of S_{41} becomes less than $\frac{1}{\sqrt{2}}$ and decrease with proportion to the stub length. From the known behavior of the S_{21} and S_{41} (makes $\frown$ shape and $\smile$ shape around the center frequency, respectively), they will intersect at two different points around the center frequency and hence increase the amplitude imbalance bandwidth. Moreover, it is observed that the change of the matching and isolation is very small and proportional to $\Delta\theta^2$.

In order to prove the concept that adding a stub and quarter wave transformers improves the bandwidth for the general case, a parametric study on the effect of the stub is carried out using the ABCD matrix circuit model with $Z_q = Z_0/\sqrt[4]{2}$, $Z_1 = Z_0$. Figure 3 shows the effect of the stub length on the amplitude imbalance of the output ports, while its effect on the matching and isolation levels is depicted in Fig. 4. Unlike the conventional rat race, which has one intersection point between the output ports, the addition of the stub provides a wide amplitude imbalance bandwidth. This is achieved by having the outputs intersect at two points instead of one. On the other hand, as the stub length increases, the separation between the intersection points increases resulting in deterioration of the output amplitude imbalance, the matching,

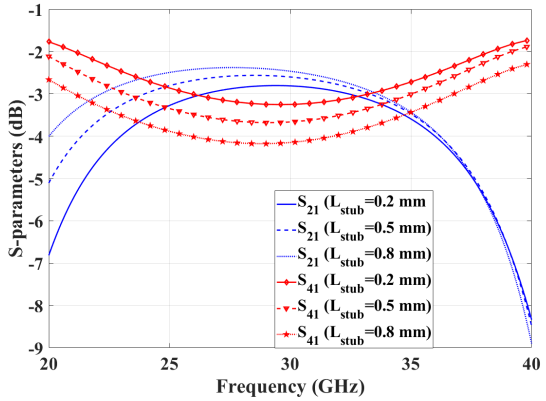

FIGURE 3. S_{21} and S_{41} of the proposed rat race with different values of L_{stub} while the other parameters are fixed ($Z_q = Z_0/\sqrt[4]{2}$, $Z_1 = Z_0$, and $Z_{stub} = 30\Omega$).

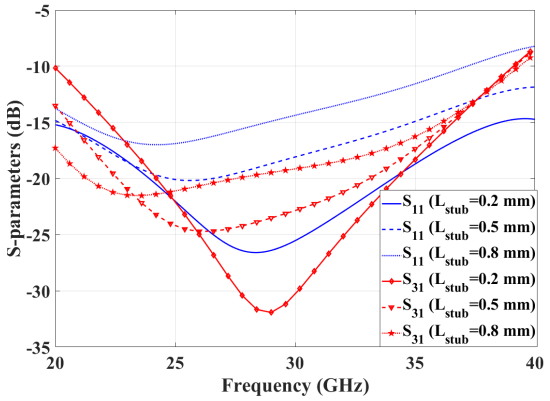

FIGURE 4. S_{11} and S_{31} of the proposed rat race with different values of L_{stub} while the other parameters are fixed ($Z_q = Z_0/\sqrt[4]{2}$, $Z_1 = Z_0$, and $Z_{stub} = 30\Omega$).

and the isolation. Therefore, optimization is needed to have a wide bandwidth with an acceptable amplitude imbalance, matching, and isolation. In this work, return loss and isolation are better than 15 dB with output ports imbalance less than 1 dB.

III. COAXIAL TO RIDGE GAP FEEDING DESIGN

The proposed device is fed by a coaxial connector. Therefore, a transition from coaxial to PRGW is designed.The unit cell of PRGW of [41] is used, where the material is Roger RT6002 ($\varepsilon_r = 2.94$ and $\tan\delta = 0.0012$) and the resulted band gap is from 22.307 to 43.095 GHz. In this work, a simplified version of the previous work [41] is introduced where the matching pins have been removed to simplify the fabrication procedure, as a moderate bandwidth (from 25 to 35 GHz) is needed. The geometry of the back-to-back configuration is shown on Fig. 5 and the associated s-parameters are shown in Fig. 6. Dimensions of the transition are in Table 1. The return loss is better than 15 dB from 25.4 GHz till 36 GHz and the associated insertion loss is higher than 0.4 dB.

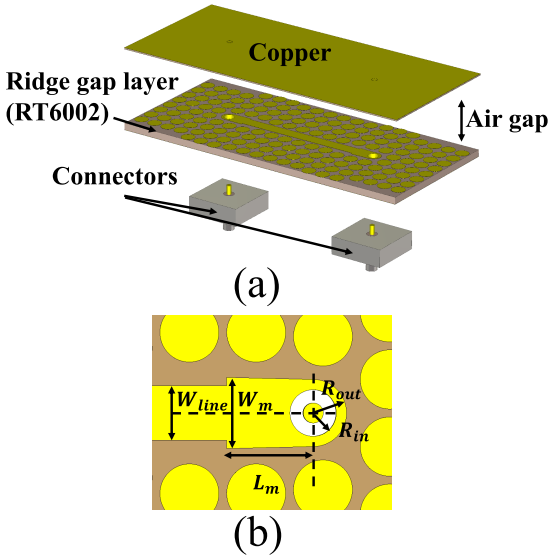

FIGURE 5. Geometry of the back-to-back configuration for a coaxial to printed ridge gap transition. (a) The whole structure. (b) details of the transition section.

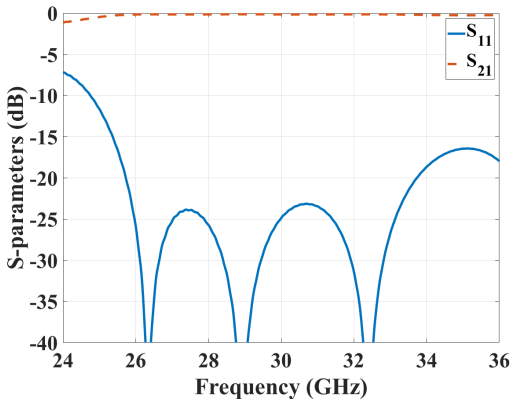

FIGURE 6. S-parameters of the back-to-back configuration for a coaxial to printed ridge gap transition.

TABLE 1. The dimensions of the coaxial to printed ridge gap transition.

Parameter	W_m	L_m	R_{in}	R_{out}	W_{line}
Value(mm)	1.8	2.2	0.59	0.85	1.38

IV. CONVENTIONAL RAT-RACE COUPLER

In this section, the conventional rat-race coupler is presented. The geometry of the structure is shown in Fig. 7, where the ring line impedance is $\sqrt{2}\ Z_0$. The lengths of the short branches are $\lambda_g/4$, and the long branch has $3\lambda_g/4$ length. The line width is 1.38 mm and the inner and outer radius of the ring coupler are $R_1 = 2.475$ mm, $R_2 = 3.325$ mm respectively. The s-parameters are shown in Fig. 8 where the bandwidth is from 28.09 to 32.4 GHz based on the previously mentioned criteria. It is clear that the bandwidth is narrow (14.25%) and also the phase difference between the differential out put ports changes rapidly,

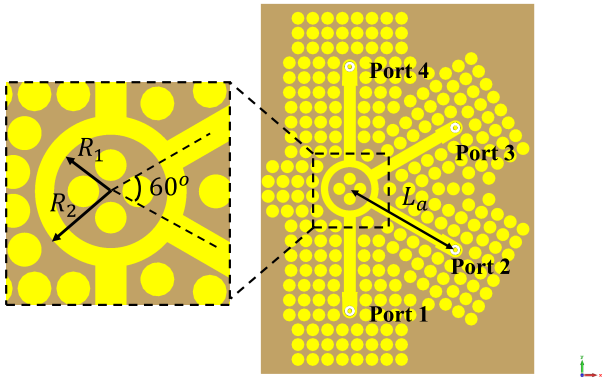

FIGURE 7. Geometry of the conventional printed ridge gap rat-race coupler.

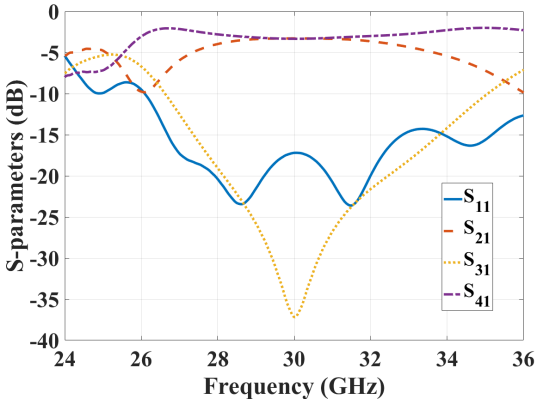

FIGURE 8. S-parameters of the conventional printed ridge gap rat-race coupler.

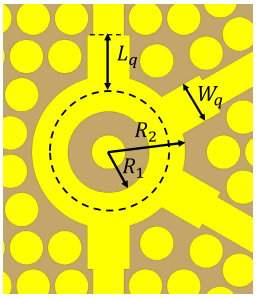

FIGURE 9. Geometry of the printed ridge gap rat-race coupler with quarter wave transformers.

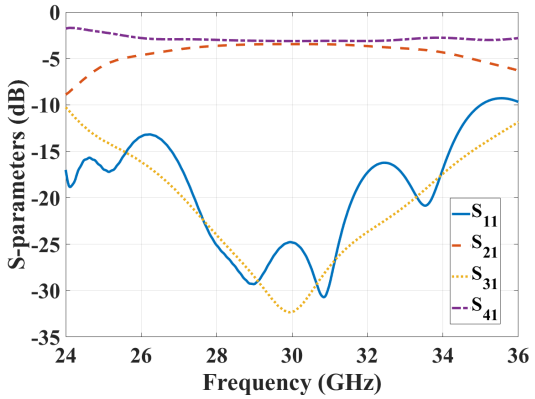

FIGURE 10. S-parameters of the printed ridge gap rat-race coupler with quarter wave transformers.

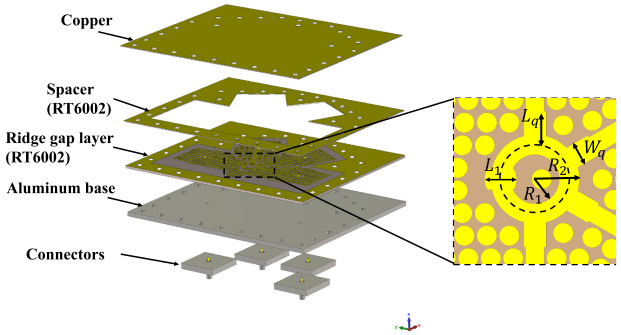

FIGURE 11. Geometry of the printed ridge gap rat-race coupler with a quarter wave transformer and a stub in the 3λ/4 branch.

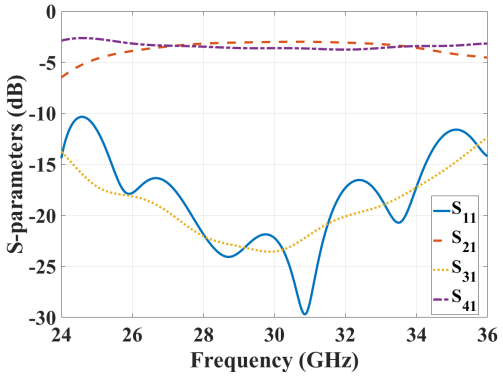

FIGURE 12. S-parameters of the printed ridge gap rat-race coupler with a quarter wave transformer and a stub.

when moving away from the center frequency as shown in Fig. 13.

V. RAT-RACE COUPLER WITH QUARTER WAVE TRANSFORMER

In order to improve the bandwidth of the rat race, quarter wave transformers are used while maintaining a 50 Ω input line impedance. The structure is shown in Fig. 9 where $W_q = 1.9$ mm, $L_q = 2.6$ mm, $R_1 = 1.8$ mm, and $R_2 = 3.4$ mm. The s-parameters are shown in Fig. 10 where the bandwidth is from 27.17 to 33.02 GHz (19.44%). It is clear that there are enhancements in both the amplitude imbalance bandwidth and the phase response (Fig. 13).

VI. RAT-RACE COUPLER WITH QUARTER WAVE TRANSFORMER AND STUB

For further improvement in the output amplitude imbalance, a stub is used in the $3/4\lambda$ branch line as perturbation to have the S_{21} and S_{31} equal to each other at two intersection points and hence a wider amplitude imbalance bandwidth.

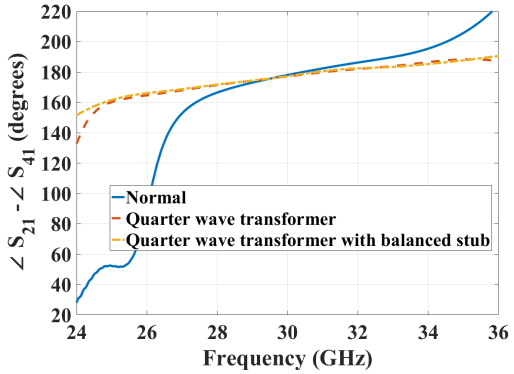

FIGURE 13. Comparison between the phase response of the rat-race coupler in the three cases: normal, with quarter wave transformer, and quarter wave transformer with stub.

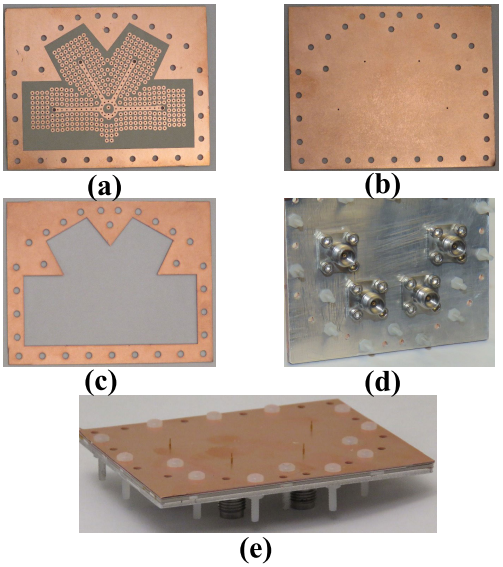

FIGURE 14. Fabricated parts. (a) ridge line layer. (b) upper copper layer. (c) Spacer layer. (d) Aluminum base with coaxial connectors. (e) Assembled 3D view.

The geometry of the coupler with the stub is shown in Fig. 11 where $W_q = 1.7$ mm, $L_q = 2.5$ mm, $R_1 = 1.85$ mm, $R_2 = 3.35$ mm, $W_{stub} = 0.8$ mm, and $L_{stub} = 2.4$ mm. The resulted s-parameters are shown in Fig. 12. The bandwidth is from 25.84 to 34.24 GHz (27.96%) which is larger than the two previous configurations. Figure 13 shows a comparison between the differential output phase response in the previous three cases. The use of quarter wavelength transformers has increased the bandwidth as well as the stability of the output phase difference.

VII. MEASUREMENT AND DISCUSSION

The fabricated prototype of the rat-race with quarter wavelength transformers and a stub is shown in Fig. 14, where the ridge line layer, the upper copper layer, and the spacer are manufactured using the conventional printed circuit board technology (PCB). The metal base (Fig. 14 (d)) has been drilled also with the PCB machining and used to hold the 2.4 coaxial connectors. The whole structure is assembled with plastic screws as shown in Fig. 14 (e). The (N52271A) PNA network analyzer has been used in measuring the s-parameters. The measured results along with the simulated ones are shown in Fig. 15 and Fig. 16 for the s-parameters amplitude and output phase difference, receptively. The behavior of the measured results matches very well with simulation results as there are two intersection points in the output ports which improve the output amplitude imbalance bandwidth, as can be seen from Fig. 17. The deviation of the measured results with the simulated ones may comes from the fabrication tolerance and the alignment mismatch.

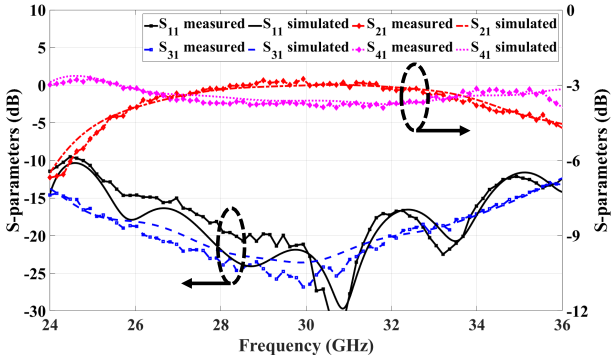

FIGURE 15. Simulated and measured s-parameters.

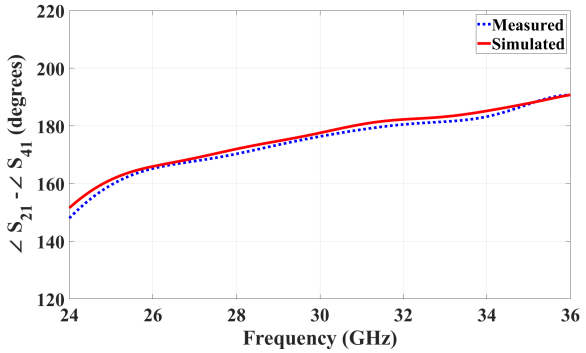

FIGURE 16. Simulated and measured output phase difference.

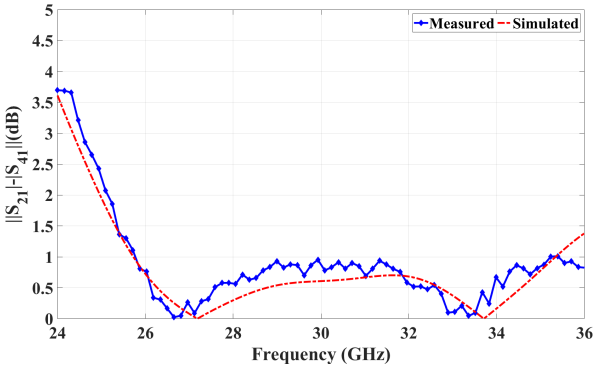

FIGURE 17. Simulated and measured output amplitude imbalance.

TABLE 2. Comparison between the proposed rat-race and other works.

	Technology	Center frequency (GHz)	Bandwidth	return loss (dB)	Isolation (dB)	amplitude imbalance (dB)	Size (ring radius+ matching)	Phase imbalance bandwidth ($180^\circ \pm 10^\circ$)
[36]	SIW	13	30%	18	20	-3.35 $\pm$1.35	15.5 mm (1.02 λ_g)	30%
[37]	HMSIW	10.15	24.6 %	12	15	-3.8 $\pm$0.5	13.2 mm (0.4962 λ_g)	24.6%
[38]	TFSIW	25.7	12.7%	20	20	-4.3 $\pm-$	3.75 mm (0.3647 λ_g)	12.45%
[39]	RSIW	8	12.5 %	12	20	-3.79 $\pm$0.5	9.1 mm (0.242 λ_0)	-
[40]	RGW	16.5	12.1%	10	20	-	5.75 mm (0.316 λ_0)	12.1%
This work	PRGW	30	27.9%	15	16.5	-3.39 $\pm$0.5	5.1 mm (0.51 λ_0)	26.6%

On Table 2, a brief comparison between the proposed coupler and other couplers is presented where the focused is on the SIW and RGW structures, as they are the promising technologies for the millimeter wave band. The proposed coupler has simultaneous both wide bandwidth and small amplitude imbalance compared to the referenced work. Moreover, it has low insertion loss as the wave propagates in an air gap region (no dielectric losses) and the structure is closed (no radiation losses). Most of the designed conventional rat-race coupler has a narrow bandwidth less than 13% [38]–[40] while the proposed one has 27.96%. In addition, SIW-based structures have higher losses compared to the proposed PRGW structure. This is due to the dielectric losses as the wave propagates in a dielectric medium while in the proposed structure, the wave propagates mainly in an air gap region. The SIW-based work in [36] and [37] are implemented in the microwave band with either a low return loss (12 dB) as in [37] or a large amplitude imbalance ($\pm$1.35 dB) as in [36].

VIII. CONCLUSION

A wideband rat-race coupler built in the PRGW technology with low amplitude imbalance and 15 dB matching and isolation levels is presented. A circuit model of the proposed rat race is presented to establish the bases for the proposed design. Then, the conventional rat-race is presented. After that, quarter wavelength transformers are used to improve the impedance matching bandwidth and the output phase difference stability. Finally, a stub is added to the $3\lambda_0/4$ branch to improve the amplitude imbalance between the output ports and to further increase the bandwidth. Moreover, a study of the effect of the added stub on both amplitude imbalance, and matching and isolation bandwidths is presented. A prototype of the last configuration is fabricated and measured. The proposed configuration has 27.96% bandwidth around 30 GHz with return loss and isolation better than 15 dB with less than 1 dB output coupling imbalance.

REFERENCES

[1] D. M. Sheen, D. L. Mcmakin, and T. E. Hall, "Three-dimensional millimeter-wave imaging for concealed weapon detection," *IEEE Trans. Microw. Theory Techn.*, vol. 49, no. 9, pp. 1581–1592, Sep. 2001.

[2] H. Zamani and M. Fakharzadeh, "1.5-D sparse array for millimeter-wave imaging based on compressive sensing techniques," *IEEE Trans. Antennas Propag.*, vol. 66, no. 4, pp. 2008–2015, Apr. 2018.

[3] Z. Briqech and A.-R. Sebak, "Millimeter-wave imaging system using a 60 GHz dual-polarized AFTSA-SC probe," in *Proc. 33rd Nat. Radio Sci. Conf. (NRSC)*, Aswan, Egypt, Feb. 2016, pp. 325–332.

[4] D. M. Sheen, J. L. Fernandes, J. R. Tedeschi, D. L. Mcmakin, A. M. Jones, W. M. Lechelt, and R. H. Severtsen, "Wide-bandwidth, wide-beamwidth, high-resolution, millimeter-wave imaging for concealed weapon detection," *Proc. SPIE*, vol. 87150, pp. 871509-1–871509-11, May 2013.

[5] A. U. Zaman, E. Rajo-Iglesias, E. Alfonso, and P.-S. Kildal, "Design of transition from coaxial line to ridge gap waveguide," in *Proc. IEEE Antennas Propag. Soc. Int. Symp.*, Charleston, SC, USA, Jun. 2009, pp. 1–4.

[6] P. S. Kildal, "Three metamaterial-based gap waveguides between parallel metal plates for mm/submm waves," in *Proc. 3rd Eur. Conf. Antennas Propag.*, Berlin, Germany, 2009, pp. 28–32.

[7] P.-S. Kildal, A. U. Zaman, E. Rajo-Iglesias, E. Alfonso, and A. Valero-Nogueira, "Design and experimental verification of ridge gap waveguide in bed of nails for parallel-plate mode suppression," *IET Microw., Antennas Propag.*, vol. 5, no. 3, pp. 262–270, 2011.

[8] H. Raza, J. Yang, P.-S. Kildal, and E. A. Alos, "Microstrip-ridge gap waveguide–study of losses, bends, and transition to WR-15," *IEEE Trans. Microw. Theory Techn.*, vol. 62, no. 9, pp. 1943–1952, Sep. 2014.

[9] A. Beltayib and A.-R. Sebak, "Analytical design procedure for forward wave couplers in RGW technology based on hybrid PEC/PMC waveguide model," *IEEE Access*, vol. 7, pp. 119319–119331, 2019.

[10] S. Birgermajer, N. Jankovic, V. Radonic, V. Crnojevic-Bengin, and M. Bozzi, "Microstrip-ridge gap waveguide filter based on cavity resonators with mushroom inclusions," *IEEE Trans. Microw. Theory Techn.*, vol. 66, no. 1, pp. 136–146, Jan. 2018.

[11] A. Beltayib, I. Afifi, and A.-R. Sebak, "4×4-element cavity slot antenna differentially-fed by odd mode ridge gap waveguide," *IEEE Access*, vol. 7, pp. 48185–48195, 2019.

[12] I. Afifi, M. M. M. Ali, and A. R. Sebak, "Analysis and design of a 30 GHz printed ridge gap Ring-crossover," in *Proc. USNC-URSI Radio Sci. Meeting (Joint AP-S Symp.)*, Atlanta, GA, USA, 2019, pp. 65–66.

[13] M. M. M. Ali, S. I. Shams, and A.-R. Sebak, "Printed ridge gap waveguide 3-dB coupler: Analysis and design procedure," *IEEE Access*, vol. 6, pp. 8501–8509, 2018.

[14] M. M. M. Ali and A.-R. Sebak, "2-D scanning magnetoelectric dipole antenna array fed by RGW butler matrix," *IEEE Trans. Antennas Propag.*, vol. 66, no. 11, pp. 6313–6321, Nov. 2018.

[15] S. M. Sifat, M. M. M. Ali, S. I. Shams, and A.-R. Sebak, "High gain bow-tie slot antenna array loaded with grooves based on printed ridge gap waveguide technology," *IEEE Access*, vol. 7, pp. 36177–36185, 2019.

[16] A. T. Hassan and A. A. Kishk, "Efficient procedure to design large finite array and its feeding network with examples of ME-dipole array and microstrip ridge gap waveguide feed," *IEEE Trans. Antennas Propag.*, to be published.

[17] D. Il Kim and Y. Naito, "Broad-band design of improved hybrid-ring 3-dB directional couplers," *IEEE Trans. Microw. Theory Techn.*, vol. MTT-30, no. 11, pp. 2040–2046, Nov. 1982.

[18] S. March, "A wideband stripline hybrid ring (Correspondence)," *IEEE Trans. Microw. Theory Techn.*, vol. MTT-16, no. 6, p. 361, Jun. 1968.

[19] R. Smolarz, K. Wincza, and S. Gruszczynski, "Impedance transforming rat-race couplers with modified lange section," *J. Electromagn. Waves Appl.*, vol. 32, no. 8, pp. 972–983, 2018, doi: 10.1080/09205071.2017.1411836.

[20] M.-H. Murgulescu, P. Legaud, E. Moisan, E. Penard, M. Goloubkoff, and I. Zaquine, "New small size, wideband 180° ring couplers: Theory and experiment," in *Proc. 24th Eur. Microw. Conf.*, Cannes, France, Sep. 1994, pp. 670–674.

[21] C.-W. Kao and C. Hsiung Chen, "Novel uniplanar 180° hybrid-ring couplers with spiral-type phase inverters," *IEEE Microw. Guided Wave Lett.*, vol. 10, no. 10, pp. 412–414, Oct. 2000.

[22] C.-W. Kao and C. H. Chen, "Miniaturized uniplanar 180° hybrid-ring couplers with 0.8 λ_g and 0.67 λ_g circumferences," in *Proc. Asia–Pacific Microw. Conf.*, Sydney, NSW, Australia, 2000, pp. 217–220.
[23] C.-H. Chi and C.-Y. Chang, "A compact wideband 180° hybrid ring coupler using a novel interdigital CPS inverter," in *Proc. Eur. Microw. Conf.*, Munich, Germany, 2007, pp. 548–551.
[24] C.-Y. Chang and C.-C. Yang, "A novel broad-band chebyshev-response rat-race ring coupler," *IEEE Trans. Microw. Theory Techn.*, vol. 47, no. 4, pp. 455–462, Apr. 1999.
[25] J. Sorocki, I. Piekarz, K. Wincza, and S. Gruszczynski, "Bandwidth improvement of rat-race couplers having left-handed transmission-line sections," *Int. J. RF Microw. Comput.-Aided Eng.*, vol. 24, no. 3, pp. 341–347, May 2014.
[26] D. Kholodnyak, P. Kapitanova, S. Humbla, R. Perrone, J. Mueller, M. A. Hein, and I. Vendik, "180° power dividers using metamaterial transmission lines," in *Proc. 14th Conf. Microw. Techn.*, Prague, Czech Republic, Apr. 2008, pp. 1–4.
[27] K. Staszek, J. Kolodziej, K. Wincza, and S. Gruszczynski, "Compact broadband rat-race coupler in multilayer technology designed with the use of artificial right- and left-handed transmission lines," *J. Telecommun. Inf. Technol.*, no. 2 pp. 107–112, 2012.
[28] J.-A. Hou and Y.-H. Wang, "Design of compact 90° and 180° couplers with harmonic suppression using lumped-element bandstop resonators," *IEEE Trans. Microw. Theory Techn.*, vol. 58, no. 11, pp. 2932–2939, Nov. 2010.
[29] G. Brzezina and L. Roy, "Miniaturized 180° hybrid coupler in LTCC for L-Band applications," *IEEE Microw. Wireless Compon. Lett.*, vol. 24, no. 5, pp. 336–338, May 2014.
[30] G. Slade, "Reduced-size octave-bandwidth microstrip/lumped-element rat-race coupler," Tech. Rep., Jun. 2008. [Online]. Available: https://www.researchgate.net/publication/229009635_Reduced-size_octave-bandwidth_microstriplumped-element_rat-race_coupler
[31] I. Haroun, Y. C. Hsu, D. C. Chang, and C. Plett, "A novel reduced-size 60-GHz 180° coupler using LG-CPW transmission lines," in *Proc. Asia–Pacific Microw. Conf.*, Melbourne, VIC, Australia, 2011, pp. 1750–1753.
[32] S. Koziel and P. Kurgan, "On elementary cell selection for miniaturized microstrip rat-race coupler design," in *Proc. Int. Conf. Electromagn. Adv. Appl. (ICEAA)*, Verona, Italy, Sep. 2017, pp. 836–839.
[33] K. V. Phani Kumar, R. K. Barik, I. S. Krishna, and S. S. Karthikeyan, "Design of compact 180° hybrid coupler for unequal power division ratio using slow wave structures," in *Proc. 23rd Nat. Conf. Commun. (NCC)*, Chennai, India, Mar. 2017, pp. 1–5.
[34] K. Sen Ang, Y. Choy Leong, and C. How Lee, "A new class of multisection 180° hybrids based on cascadable hybrid-ring couplers," *IEEE Trans. Microw. Theory Techn.*, vol. 50, no. 9, pp. 2147–2152, Sep. 2002.
[35] W. Che, K. Deng, E. K. N. Yung, and K. Wu, "H-plane 3-dB hybrid ring of high isolation in substrate-integrated rectangular waveguide (SIRW)," *Microw. Opt. Technol. Lett.*, vol. 48, no. 3, pp. 502–505, Mar. 2006.
[36] R. Dehdasht-Heydari, K. Forooraghi, and M. Naser-Moghadasi, "Efficient and accurate analysis of a substrate integrated waveguide (SIW) rat-race coupler excited by four U-shape slot-coupled transitions," *Appl. Comput. Electromagn. Soc. J.*, vol. 30, no. 1, pp. 42–49, 2015.
[37] X. Zou, C.-M. Tong, C.-Z. Li, and W.-J. Pang, "Wideband hybrid ring coupler based on half-mode substrate integrated waveguide," *IEEE Microw. Wireless Compon. Lett.*, vol. 24, no. 9, pp. 596–598, Sep. 2014.
[38] Y. Ding and K. Wu, "Miniaturized hybrid ring circuits using T-type folded substrate integrated waveguide (TFSIW)," in *IEEE MTT-S Int. Microw. Symp. Dig.*, Boston, MA, USA, Jun. 2009, pp. 705–708.
[39] A. A. M. Ali, H. B. El-Shaarawy, and H. Aubert, "Miniaturized hybrid ring coupler using electromagnetic bandgap loaded ridge substrate integrated waveguide," *IEEE Microw. Wireless Compon. Lett.*, vol. 21, no. 9, pp. 471–473, Sep. 2011.
[40] J. Yang and H. Raza, "Empirical formulas for designing gap-waveguide hybrid ring coupler," *Microw. Opt. Technol. Lett.*, vol. 55, no. 8, pp. 1917–1920, Aug. 2013.
[41] I. Afifi, M. M. M. Ali, and A.-R. Sebak, "Analysis and design of a wideband coaxial transition to metal and printed ridge gap waveguide," *IEEE Access*, vol. 6, pp. 70698–70706, 2018.
[42] M. D. Pozar, *Microwave Engineering*, 4th ed. Hoboken, NJ, USA: Wiley, 2011.

ISLAM AFIFI (Graduate Student Member, IEEE) received the B.Sc. degree in electronics and communication engineering and the M.Sc. degree in engineering physics from Cairo University, Cairo, Egypt, in 2009 and 2014, respectively. He is currently pursuing the Ph.D. degree in electrical and computer engineering with Concordia University, Montreal, QC, Canada. He was a Teaching and a Research Assistant with the Engineering Mathematics and Physics Department, from 2009 to 2014, and a Senior Teaching Assistant, from 2014 to 2016. His research interest includes millimeter-wave microwave components and antennas.

ABDEL RAZIK SEBAK (Life Fellow, IEEE) received the B.Sc. degree (Hons.) in electrical engineering from Cairo University, Cairo, Egypt, in 1976, the B.Sc. degree in applied mathematics from Ein Shams University, Cairo, in 1978, and the M.Eng. and Ph.D. degrees in electrical engineering from the University of Manitoba, Winnipeg, MB, Canada, in 1982 and 1984, respectively. From 1984 to 1986, he was with Canadian Marconi Company involving in the design of microstrip phased array antennas. From 1987 to 2002, he was a Professor with the Department of Electronics and Communication Engineering, University of Manitoba. He is currently a Professor with the Department of Electrical and Computer Engineering, Concordia University, Montreal, QC, Canada. His research interests include phased array antennas, millimeter-wave antennas and imaging, computational electromagnetics, and interaction of EM waves with engineered materials and bioelectromagnetics. He is a member of the Canadian National Committee of International Union of Radio Science Commission B. He was a recipient of the 2000 and 1992 University of Manitoba Merit Award for outstanding Teaching and Research, the 1994 Rh Award for Outstanding Contributions to Scholarship and Research, and the 1996 Faculty of Engineering Superior. He has served as the Chair of the IEEE Canada Awards and Recognition Committee from 2002 to 2004, and the Technical Program Chair of the 2002 IEEE CCECE Conference and the 2006 URSIANTEM Symposium. He is also the Technical Program Co-Chair for the 2015 IEEE ICUWB Conference.